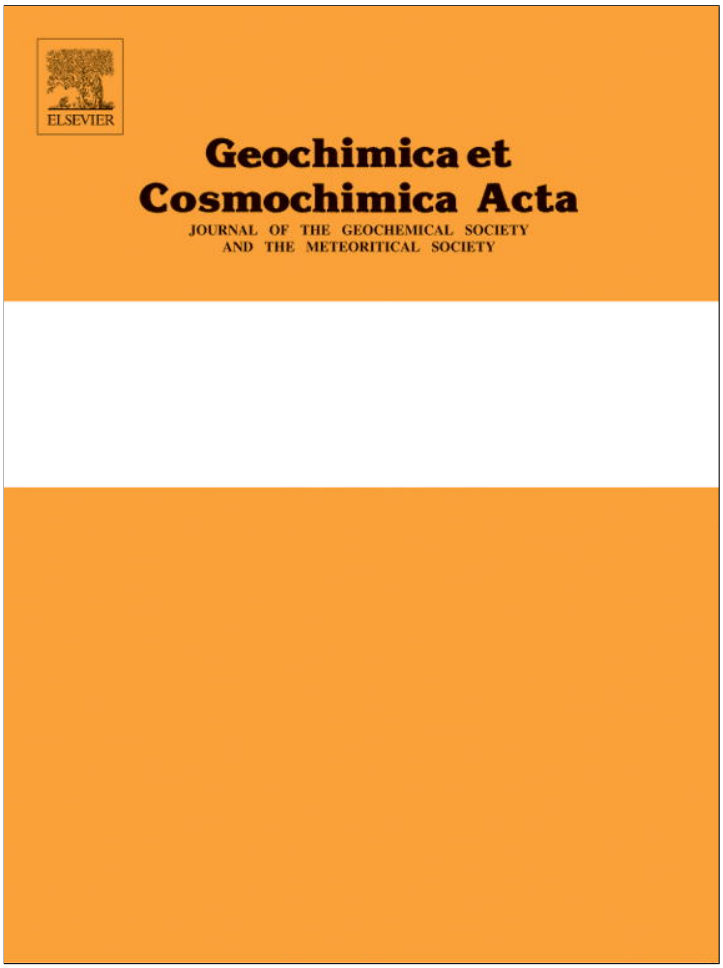

(This is a sample cover image for this issue. The actual cover is not yet available at this time.)

Available online at www.sciencedirect.com

SciVerse ScienceDirect

Geochimica et Cosmochimica Acta 95 (2012) 134–142

Geochimica et Cosmochimica Acta

www.elsevier.com/locate/gca

Important role of colloids in the cycling of ^{210}Po and ^{210}Pb in the ocean: Results from the East/Japan Sea

Tae-Hoon Kim, Guebuem Kim *

School of Earth and Environmental Sciences/RIO, Seoul National University, Seoul 151-747, Republic of Korea

Received 28 January 2012; accepted in revised form 23 July 2012

Abstract

The activities of ^{210}Pb and ^{210}Po were measured for the truly dissolved (<10 kDa), colloidal (10 kDa–0.45 μm), and particulate (>0.45 μm) phases in the upper ocean (0–200 m) of the East/Japan Sea (EJS) in the summer of 2009. We report, for the first time, data on truly dissolved and colloidal ^{210}Pb and ^{210}Po in the ocean. The total ^{210}Pb and ^{210}Po activities in the EJS were in the ranges of 6.3–23 dpm/100L and 3.3–10 dpm/100L, respectively. In the upper ocean, the proportions of the truly dissolved, colloidal, and particulate phases were, respectively, $35 \pm 3\%$, $48 \pm 7\%$, and $17 \pm 8\%$ for ^{210}Pb and $19 \pm 2\%$, $36 \pm 6\%$, and $45 \pm 6\%$ for ^{210}Po. Using a net residence time model, which accounts for biological uptake and remineralization, the residence times of ^{210}Po in the upper 100-m layer were calculated to be 92 ± 41, 63 ± 14, and 166 ± 45 days for the truly dissolved, colloidal, and particulate phases, respectively. The residence time of colloidal ^{210}Po was several-fold longer than typical turnover times (<10 days) of high-molecular-weight dissolved organic carbon and colloidal residence times of short-lived ^{234}Th in the surface water. This result suggests that ^{210}Po turns over several times through the colloidal phase, perhaps together with other bio-reactive elements, before settling down from the upper ocean.

1. INTRODUCTION

Both ^{210}Pb (half-life 22.3 years) and ^{210}Po (half-life 138 days) belong to the ^{238}U decay series. ^{210}Pb is produced by ^{226}Ra decay via short-lived daughters, including the chemically inert noble gas ^{222}Rn (half-life 3.8 days). ^{210}Po is produced by ^{210}Pb decay via the short-lived intermediate ^{210}Bi (half-life 5 days). Thus, in the upper ocean, ^{210}Pb originates from both the atmosphere and in situ production, while most ^{210}Po is produced by the in situ decay of ^{210}Pb. Both ^{210}Pb and ^{210}Po are removed by adsorption onto particulate matter in seawater, but ^{210}Po is more efficiently taken up and removed by biota (Fisher et al., 1983; Kadko, 1993; Wei and Murray, 1994; Kim, 2001; Stewart et al., 2005). This preferential uptake of ^{210}Po by marine biota causes significant radioactive disequilibria between ^{210}Pb and ^{210}Po in the upper ocean (Bacon et al., 1988; Kadko, 1993; Kim, 2001).

Although ^{210}Po removal is known to be associated with biological production in the water column, large deficiencies in ^{210}Po have been observed in oligotrophic areas of the ocean, such as the East China Sea (Nozaki et al., 1990), the Sargasso Sea (Kim, 2001), and the northern South China Sea (Chung and Wu, 2005). Nozaki et al. (1990) have shown that such large deficiencies in the East China Sea are due to the focused input of atmospheric ^{210}Pb rather than preferential scavenging of ^{210}Po. However, Kim (2001) and Chung and Wu (2005) have suggested that such large deficiencies in ^{210}Po in the oligotrophic ocean are likely to occur because of the effective uptake of ^{210}Po by organisms such as cyanobacteria (i.e., *Tricodesium*), which are then transferred to the higher trophic levels through the food web. In the eutrophic ocean, however, ^{210}Po may be released into the water through rapid decomposition or remineralization of organic matter, particularly below the mixed layer, resulting in a relatively small deficiency or even an excess (Kim, 2001).

* Corresponding author. Tel.: +82 2 880 7508; fax: +82 2 876 6508.

E-mail address: gkim@snu.ac.kr (G. Kim).

0016-7037/$ - see front matter © 2012 Elsevier Ltd. All rights reserved.
http://dx.doi.org/10.1016/j.gca.2012.07.029

Nevertheless, ^{210}Pb and ^{210}Po have been successfully used for studying particle scavenging and vertical fluxes (Cherry et al., 1975; Cochran et al., 1983; Fowler and Knauer, 1986; Nozaki et al., 1997; Masqué et al., 2002) and particulate organic carbon (POC) export (Shimmield et al., 1995; Friedrich and Rutgers van der Loeff, 2002; Murray et al., 2005; Stewart et al., 2010) in the upper ocean. However, there is no information on the role of colloids in the cycling of ^{210}Pb and ^{210}Po in the ocean although marine colloids are known to play an important role in the biogeochemical cycling of many particle-reactive nuclides (Guo and Santschi, 1997).

Thus, in this study, we have (1) determined colloidal ^{210}Pb and ^{210}Po activities in the open ocean, for the first time, (2) calculated the residence time of the truly dissolved, colloidal, and particulate phases of ^{210}Po in the euphotic zone as possible proxies for other bio-reactive elements in the ocean, and (3) evaluated the biogeochemical factors controlling the partitioning and residence times of ^{210}Po in the ocean. We used 10 kDa, instead of 1 kDa, cut-off size for colloidal separations in order to trace the turnover rate of ^{210}Po in higher molecular weight colloidal fraction which turns over on timescale of <1 year, suitable for the half-life of ^{210}Po. In general, lower molecular weight colloidal fraction (e.g., 1–10 kDa) turns over on timescales of >10 years (Guo and Santschi, 1997).

2. MATERIALS AND METHODS

2.1. Study area

The East/Japan Sea (EJS) in the Northwest Pacific Ocean is a typical semi-closed marginal sea with a surface area of 1.01×10^6 km^2 and a maximum depth of >3700 m. Because it has its own deep convection system (thermohaline conveyor belt), which is independent of the Pacific Ocean, the EJS has been regarded as a miniature of the global ocean in terms of deep water formation (Kim et al., 2001, 2002; Gamo et al., 2001). The EJS water is separated into colder water (North Korea Cold Current) to the north and warmer and more saline water to the south (Tsushima Warm Current). The confluence of the two currents forms the Polar Front generally located south of 40°N (Hong and Cho, 1983; Rebstock and Kang, 2003; Park et al., 2004; Kim et al., 2010). The water residence time of the EJS is about 100 years (Tsunogai et al., 1993; Kim et al., 2001).

2.2. Sampling

Sampling was conducted during two periods: (1) July 9–18, 2009, on *R*/*V* M. A. Lavrentyev of the Pacific Oceanological Institute (POI), Russia; (2) August 8–18, 2009, on *R*/*V* HaeYang 2000 of the National Oceanographic Research Institute (NORI), Korea (Fig. 1). Seawater samples were collected at two stations in the northern part of the EJS during July 9–18, 2009, and at one station in the southern part of the EJS during August 8–18, 2009. Niskin bottles mounted on a rosette system (equipped with CTD SBE 911plus) were used for vertical water sampling.

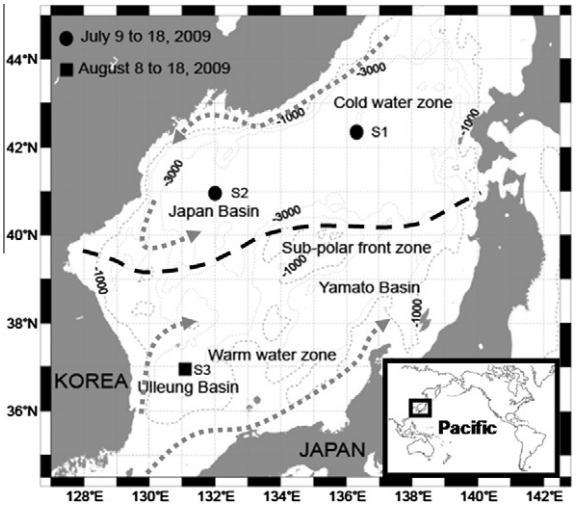

Fig. 1. Map showing sampling stations for ^{210}Pb and ^{210}Po in the East/Japan Sea.

After sample collection, about 500 mL of the water samples was filtered with a Whatman disposable syringe filter equipped with a GF/F filter for dissolved organic carbon (DOC) analyses, and 1 L of the water samples was filtered through a Whatman GF/F onboard the ship for chlorophyll *a* analyses. The DOC samples were stored in fire-sealed pre-combusted (500 °C for 4 h) glass ampoules after 6 M HCl had been added to acidify the samples below pH 2. GF/F filters for chlorophyll *a* were stored in a deep freezer (−80 °C) immediately after filtration.

For the ^{210}Pb and ^{210}Po analyses, 20 L of seawater was filtered immediately after sampling using a cellulose membrane filter (Millipore) to separate the total dissolved fraction (<0.45 μm) and the particulate fraction. Thereafter, 10 L of the total dissolved fraction was used to separate the colloidal (10 kDa–0.45 μm) and truly dissolved (<10 kDa) fractions using a tangential flow filtration (TFF) system (PLCGC, Pellicon). Before and after use, the TFF cartridge was cleaned rigorously using 1 M HCl (20 min), 10 L of deionized water, 0.5 M NaOH, and 10 L of deionized water (Gueguen et al., 2002; Baskaran et al., 2003). The flow rate of the tangentially circulating fluid in the membrane was about 1 L/min for the permeate, which is the truly dissolved fraction passing through the TFF membrane. Filtration was completed onboard within 10 h of sampling in order to minimize particle sinkage, decomposition, and adsorption onto the walls of the sampling bottles. The filtered water samples were stored in acid-cleaned plastic containers after the pH had been adjusted to less than 2.

In order to determine the retention coefficient (*R*) of a 10 kDa cartridge, two macromolecular organic compounds (cytochrome C and vitamin B-12) with known molecular weights (MW) were used in the laboratory experiments. The size of the ultrafilter cutoff is slightly lower than that (12 kDa) of cytochrome C, but higher than that (1.3 kDa) of vitamin B-12. The concentration factor (12.5 for cytochrome C and 11.1 for vitamin B-12) was calculated from the ratio of the initial volume to the retentate volume,

and initial DOC concentrations for both of them (cytochrome C and vitamin B-12) were about 100 μM. The *R* values of the TFF system using a DOC mass balance were about 94% and 29% for cytochrome C and vitamin B-12, respectively, and these values were similar to those reported by Guo and Santschi (1996) and considered acceptable for our purposes. The recovery efficiencies of the TFF system for ^{210}Pb and ^{210}Po were obtained by comparing the combined activities of the truly dissolved and colloidal fractions with the activities of the total dissolved fraction. The recovery efficiencies for ^{210}Pb and ^{210}Po varied from 90 ± 6% to 118 ± 8% for 24 samples (Table 1), within the uncertainties of our chemical separation and activity counting.

2.3. ^{210}Po, ^{210}Pb, chlorophyll *a*, and DOC analyses

The chemical procedures for the analyses of ^{210}Pb and ^{210}Po were modified from those of Kim et al. (1999a). The samples were spiked with 1 dpm of ^{209}Po, 25 mg of the Pb^{2+} carrier, and 75 mg of the Fe^{3+} carrier. After vigorous stirring for 10 min, the samples were allowed to stand overnight to ensure complete equilibration between the spike and the carriers. Thereafter, the pH of the samples was adjusted using a solution of ammonia (NH_4OH) in order to co-precipitate Pb and Po with $Fe(OH)_3$ at pH 8. After allowing the precipitate to settle for another 6 h, the supernatant was discarded. The precipitate was then filtered through Whatman grade 41 quantitative paper and dissolved in HCl. This sample solution was brought back to the laboratory for further analyses. In the laboratory, the solution was transferred to a Teflon beaker, and the organic matter was completely digested with concentrated HCl, HNO_3, and HF, and then converted to 0.5 M HCl. After adding 0.5 g of ascorbic acid, the solution was heated to 90 °C, and Po was spontaneously plated onto a silver disc. The alpha particles of ^{210}Po were counted using a passivated implanted planar silicon (PIPS) detector.

After the self-plating of Po onto the disc, the solution was dried and then dissolved in 5 mL of 9 M HCl. Pb was separated from the Po using a preconditioned 9 M HCl anion-exchange column (AG 1 × 8 resin, 100–200 mesh). The remaining Po was adsorbed in the column, while Pb passed through the column. Once a ^{209}Po spike had been added to the collected Pb solution, the sample was stored in a clean plastic bottle for more than 3 months. The ^{210}Pb activity was measured by determining the in-grown activity of ^{210}Po. The chemical yield of Pb from the overall procedure was determined by measuring the stable Pb recovery for an aliquot of the ^{210}Pb solution.

Table 1
Recovery of ^{210}Pb and ^{210}Po using tangential flow filtration.

Station	Depth (m)	Recovery rate (%)	
		^{210}Pb	^{210}Po
S1	0	99 ± 4	118 ± 8
	50	90 ± 6	105 ± 12
	100	103 ± 8	107 ± 11
	200	106 ± 8	107 ± 12
S2	0	105 ± 5	106 ± 7
	50	104 ± 7	117 ± 13
	100	110 ± 8	103 ± 10
	200	107 ± 8	110 ± 11
S3	0	103 ± 4	96 ± 3
	50	101 ± 5	95 ± 6
	100	101 ± 6	109 ± 5
	200	96 ± 4	106 ± 5

The frozen filters for chlorophyll *a* were extracted in 5 ml of 100% acetone with an internal standard (50 μL canthaxanthin) at −20 °C for 24 h in the dark, sonicated for 30 s, and then centrifuged for 10 min at 2000 rpm to remove cellular and filter debris. Acetone extracts were determined for pigments by HPLC using a modified version of the method described by Wright et al. (1991). In brief, the supernatant was filtered through a 0.45 μm PTFE syringe filter, and the clear extract (1 mL) was mixed with deionized water (0.3 mL). The mixed solution (0.1 mL) was injected into a HPLC system (Waters 2695, Waters Co.).

Concentrations of DOC were measured using a TOC-V_{CPH} (Shimadzu, Japan). Five-point standard curves of acetanilide were used to standardize the DOC measurements. High-purity air (purity: 99.999%) was bubbled through the acidified seawater samples to completely purge inorganic carbon species from the injection system. The carrier gas was passed at a controlled flow rate of 150 mL min^{-1} through a combustion tube that was filled with a thermal decomposition catalyst and heated to 720 °C. The samples of DOC were oxidized to produce CO_2. This CO_2 was detected by an NDIR detector. The reliability of measurements was checked daily by comparison with the DOC certified seawater sample (DSR: 44–46 μM for DOC, University of Miami). The results agreed with the certified value within 5%.

3. RESULTS AND DISCUSSION

3.1. Distributions of temperature, chlorophyll *a*, DOC, ^{210}Pb, and ^{210}Po

Temperatures decreased steeply from 26 to 1 °C in the surface layer (0–100 m) (Fig. 2). The mixed layer depth was within 10 m in the study region. The concentrations of chlorophyll *a* were in the range of 10–1130 ng/L in the surface layer. The highest concentrations of chlorophyll *a* were observed at depths between 25 and 50 m (Fig. 2). The concentrations of DOC in the upper 200-m layer were in the range of 64–86 μM (Fig. 2), which were similar to those in the world's major oceans (Carlson and Ducklow, 1995; Hansell and Carlson, 1998). The concentrations of DOC were highest in the surface layer and decreased with depth.

The total activities of ^{210}Pb decreased with increasing depth in the EJS (Fig. 2), as observed for other areas of the open ocean (Bacon et al., 1988; Nozaki et al., 1990; Kim, 2001; Chung and Wu, 2005) in association with major source inputs from the atmosphere (Fig. 2). The total ^{210}Pb activities in the surface water of the northern region (S1 and S2) were about 40% higher than those of the southern region (S3), perhaps due to Asian dusts passing through the

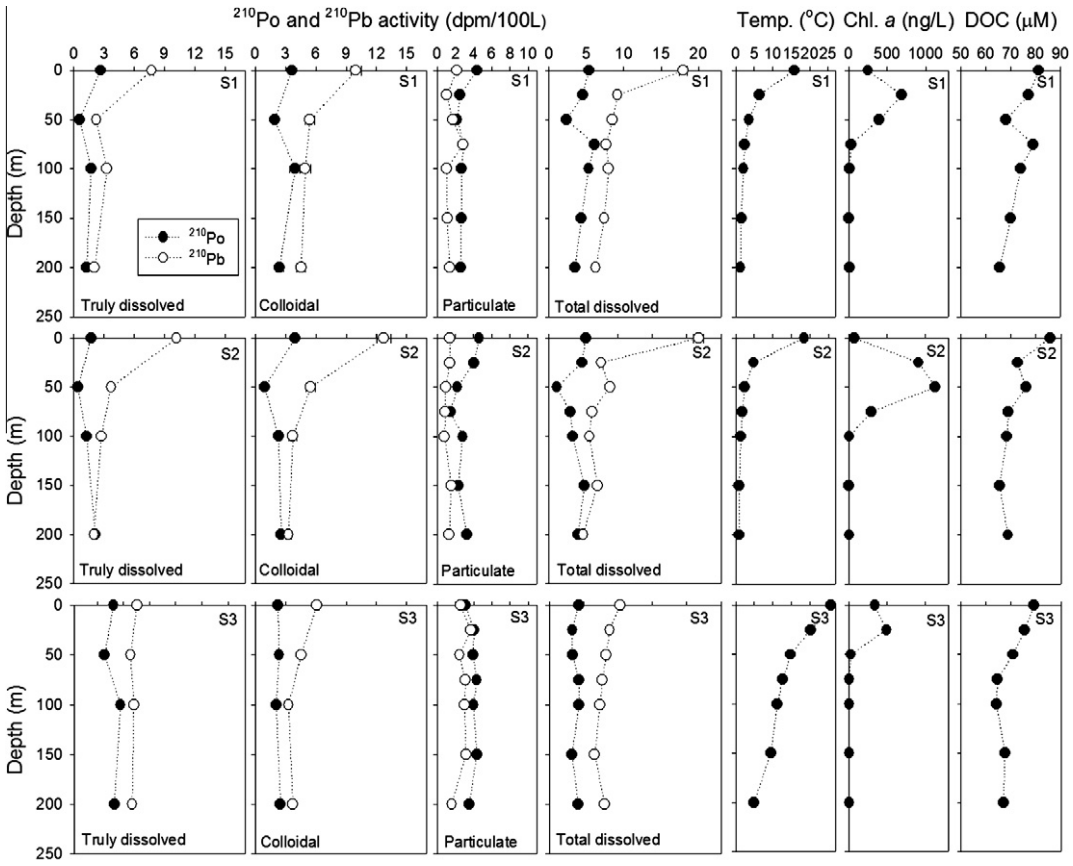

Fig. 2. Vertical profiles of temperature, chlorophyll *a*, DOC, and the activities of ^{210}Pb (open circles) and ^{210}Po (closed circles) in the truly dissolved (<10 kDa), colloidal (10 kDa–0.45 μm), particulate (>0.45 μm), and total dissolved (<0.45 μm) phases in the East/Japan Sea.

northern area of the EJS (Jo et al., 2007). These activities in the northern region are similar to those in the North Pacific (20–27 dpm/100L) (Nozaki et al., 1976, 1990). The total activities of ^{210}Po were 20–70% lower than those of ^{210}Pb at all stations (Fig. 2), with larger ^{210}Po deficits in the euphotic zone. Such disequilibrium patterns have been commonly found in other areas of the ocean, such as in the Kuroshio Current (Nozaki et al., 1990), the Sargasso Sea (Kim, 2001), and the northern South China Sea (Chung and Wu, 2005) and are known to be associated with the preferential uptake of ^{210}Po by marine organisms (Cochran et al., 1983; Stewart and Fisher, 2003a; Stewart et al., 2005).

In the total dissolved (truly dissolved + colloidal) phase, ^{210}Po activities were much lower than ^{210}Pb activities at all stations. For both ^{210}Pb and ^{210}Po, the activities and the vertical distribution patterns of the truly dissolved phase were similar to those of the colloidal phase (Fig. 2). Of the total activities, the truly dissolved phase constituted 32–38% (avg.: 35%) for ^{210}Pb and 17–20% (avg.: 19%) for ^{210}Po; the colloidal phase constituted 39–53% (avg.: 48%) for ^{210}Pb and 29–42% (avg.: 36%) for ^{210}Po. The proportions of the truly dissolved and colloidal phases were somewhat lower for ^{210}Po than for ^{210}Pb. The activities of the total dissolved ^{210}Pb decreased with increasing depth in the EJS (Fig. 2) in association with atmospheric source inputs, while the activities of the total dissolved ^{210}Po were lowest in the layer with the maximum chlorophyll *a* concentration (25–50 m). Although the ^{210}Po deficits were largest at station S2, where chlorophyll *a* concentrations were highest, the correlation between the concentrations of chlorophyll *a* (an indicator of the biomass of the water column) and the deficiency of the truly dissolved and colloidal ^{210}Po showed a large scatter (Fig. 3). This scatter may be due to different removal efficiency of ^{210}Po by different organisms and/or time-lapses between the ^{210}Po removal and biological production/export.

Particulate ^{210}Pb and ^{210}Po showed almost uniform activities over the entire depth range (Fig. 2). The particulate phases of total ^{210}Pb and ^{210}Po constituted 11–26% (avg.: 17%) and 38–51% (avg.: 45%), respectively. The particulate ^{210}Po activity was slightly higher than the particulate ^{210}Pb activity, similar to observations in the open oceans in association with preferential Po uptake by biota (e.g., Bacon et al., 1976; Chung and Craig, 1983; Chung, 1987; Chung and Finkel, 1988).

3.2. Residence times of ^{210}Po

A steady-state model was used for estimating the residence times of ^{210}Po in the open oceans (Fig. 4). This steady-state model assumes that vertical mixing, advection, and diffusion terms are negligible relative to a removal term. In these well-stratified water columns (Fig. 2), the assumptions may be valid as shown in other areas of the oceans for

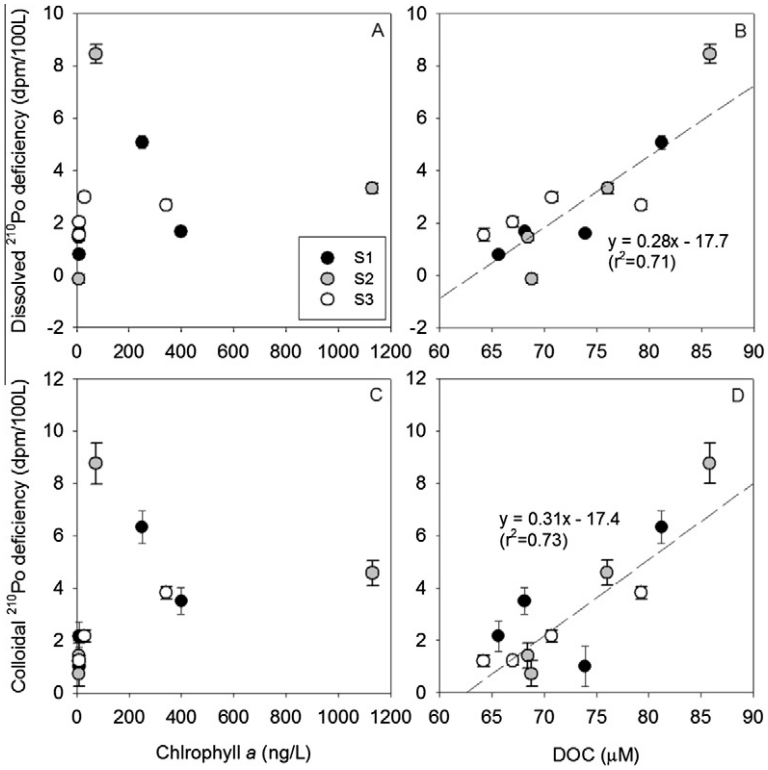

Fig. 3. ^{210}Po deficiencies in the truly dissolved and colloidal phases versus chlorophyll *a* (A and C) and DOC (B and D) in the East/Japan Sea.

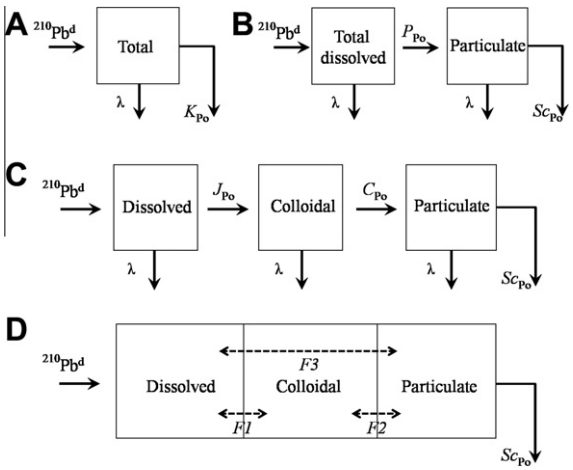

Fig. 4. Box model schemes for removal of ^{210}Po from the ocean. (A–C) The sequential scavenging models used to calculate the residence times of ^{210}Po: (A) the net removal flux out from the box (K_{Po}), (B) the scavenging flux from the total dissolved to particulate phase (P_{Po}) and the settling flux of particulates (Sc_{Po}), (C) the scavenging fluxes from the truly dissolved to colloidal phase (J_{Po}), from the colloidal to particulate phase (C_{Po}), and Sc_{Po}, and (D) the net residence time model used to account for biological uptake and remineralization of ^{210}Po. λ is the decay constant of ^{210}Po; *F1*, *F2*, and *F3* represent the net removal fluxes of ^{210}Po.

particle-reactive elements such as Th and Po (Coale and Bruland, 1987; Sarin et al., 1999; Kim and Church, 2001). There may be additional errors in this model occurring from episodic fallouts of atmospheric ^{210}Pb (with a large deficit of ^{210}Po). The interactions between the colloidal and particulate phases were simplified to an irreversible sequential process, with a transfer to the next larger size class. This sequential scavenging model (Bacon et al., 1976) can be expressed as follows:

For ^{210}Po,

$$\frac{\partial A^{\mathrm{tot}}}{\partial \mathrm{t}} = 0 = (I_{\mathrm{P}}^{\mathrm{tot}} - I_{\mathrm{D}}^{\mathrm{tot}}) \times \lambda - \mathrm{K} \quad (1)$$

$$\frac{\partial A^{\mathrm{tdis}}}{\partial t} = 0 = (I_{\mathrm{P}}^{\mathrm{tdis}} - I_{\mathrm{D}}^{\mathrm{tdis}}) \times \lambda - \mathrm{P} \quad (2)$$

$$\frac{\partial A^{\mathrm{dis}}}{\partial t} = 0 = (I_{\mathrm{P}}^{\mathrm{dis}} - I_{\mathrm{D}}^{\mathrm{dis}}) \times \lambda - \mathrm{J} \quad (3)$$

$$\frac{\partial A^{\mathrm{col}}}{\partial t} = 0 = (I_{\mathrm{P}}^{\mathrm{col}} - I_{\mathrm{D}}^{\mathrm{col}}) \times \lambda + J - C \quad (4)$$

$$\frac{\partial A^{\mathrm{par}}}{\partial t} = 0 = (I_{\mathrm{P}}^{\mathrm{par}} - I_{\mathrm{D}}^{\mathrm{par}}) \times \lambda + C - Sc \quad (5)$$

where $I_P^{\mathrm{tot,tdis,dis,col,par}}$ and $I_D^{\mathrm{tot,tdis,dis,col,par}}$ are the inventories of the total, total dissolved, truly dissolved, colloidal, and particulate phases of ^{210}Pb and ^{210}Po, respectively. *K*, *P*, *J*, *C*, and S_c are, respectively, the removal fluxes for the total, total dissolved, truly dissolved, colloidal, and particulate phases of ^{210}Po, and λ denotes the decay constant for ^{210}Po. In this study, the inventories for the truly dissolved and colloidal phases were calculated by using data from depths of 0, 50, and 100 m, and those for the total dissolved and particulate phases were calculated by using data from depths of 0, 25, 50, 75, and 100 m (Table 2).

Table 2
Distributions of total, total dissolved, truly dissolved, colloidal, and particulate phases of ^{210}Pb and ^{210}Po in East/Japan Sea.

Station	Depth (m)	Total		Total dissolved (<0.45 μm)		Truly dissolved (<10 kDa)		Colloid (10 kDa–0.45 μm)		Particulate (>0.45 μm)	
		^{210}Pb	^{210}Po	^{210}Po	^{210}Po	^{210}Pb	^{210}Po	^{210}Pb	^{210}Po	^{210}Pb	^{210}Po
S1	0	20.2 ± 0.5	9.8 ± 0.2	18.0 ± 0.5	5.4 ± 0.2	7.7 ± 0.2	2.7 ± 0.1	10.0 ± 0.5	3.6 ± 0.4	2.2 ± 0.1	4.4 ± 0.1
	25	10.2 ± 0.1	6.0 ± 0.2	9.2 ± 0.1	4.5 ± 0.2	–	–	–	–	1.0 ± 0.1	2.5 ± 0.1
	50	10.2 ± 0.3	4.6 ± 0.1	8.5 ± 0.3	2.4 ± 0.1	2.2 ± 0.1	0.6 ± 0.1	5.4 ± 0.4	1.9 ± 0.2	1.7 ± 0.1	2.2 ± 0.1
	75	10.6 ± 0.2	7.0 ± 0.2	7.7 ± 0.2	6.1 ± 0.2	–	–	–	–	2.9 ± 0.1	2.9 ± 0.1
	100	9.1 ± 0.2	8.0 ± 0.2	8.0 ± 0.2	5.3 ± 0.2	3.3 ± 0.1	1.7 ± 0.1	5.0 ± 0.3	4.0 ± 0.5	1.1 ± 0.1	2.7 ± 0.1
	150	8.5 ± 0.2	6.9 ± 0.2	7.4 ± 0.2	4.3 ± 0.2	–	–	–	–	1.1 ± 0.1	2.6 ± 0.1
	200	7.7 ± 0.2	6.1 ± 0.2	6.3 ± 0.2	3.5 ± 0.2	2.1 ± 0.1	1.3 ± 0.1	4.6 ± 0.4	2.4 ± 0.4	1.4 ± 0.1	2.6 ± 0.1
S2	0	23.2 ± 0.7	10.0 ± 0.2	21.8 ± 0.7	5.4 ± 0.2	10.2 ± 0.4	1.7 ± 0.1	12.7 ± 0.7	4.0 ± 0.3	1.4 ± 0.1	4.6 ± 0.2
	25	14.0 ± 0.3	8.8 ± 0.3	7.6 ± 0.3	4.8 ± 0.2	–	–	–	–	1.4 ± 0.1	4.0 ± 0.2
	50	9.8 ± 0.3	3.3 ± 0.1	8.8 ± 0.3	1.1 ± 0.1	3.7 ± 0.2	0.4 ± 0.0	5.5 ± 0.5	0.9 ± 0.1	1.0 ± 0.1	2.2 ± 0.1
	75	7.1 ± 0.2	4.6 ± 0.1	6.2 ± 0.2	3.1 ± 0.1	–	–	–	–	0.9 ± 0.1	1.5 ± 0.1
	100	6.7 ± 0.2	6.3 ± 0.1	5.9 ± 0.2	3.5 ± 0.1	2.7 ± 0.1	1.3 ± 0.1	3.7 ± 0.4	2.3 ± 0.3	0.8 ± 0.1	2.8 ± 0.1
	150	8.5 ± 0.3	7.4 ± 0.2	7.0 ± 0.3	5.1 ± 0.1	–	–	–	–	1.5 ± 0.1	2.3 ± 0.1
	200	6.3 ± 0.2	7.6 ± 0.2	5.0 ± 0.2	4.3 ± 0.2	2.0 ± 0.1	2.1 ± 0.1	3.3 ± 0.3	2.6 ± 0.4	1.3 ± 0.1	3.3 ± 0.1
S3	0	12.8 ± 0.3	7.4 ± 0.2	10.3 ± 0.3	4.3 ± 0.2	4.5 ± 0.2	1.9 ± 0.1	6.1 ± 0.2	2.3 ± 0.1	2.5 ± 0.1	3.1 ± 0.1
	25	12.5 ± 0.3	7.4 ± 0.2	8.8 ± 0.3	3.4 ± 0.1	–	–	–	–	3.7 ± 0.2	4.0 ± 0.2
	50	10.7 ± 0.3	7.3 ± 0.2	8.3 ± 0.3	3.4 ± 0.2	3.8 ± 0.2	0.9 ± 0.1	4.5 ± 0.1	2.4 ± 0.1	2.4 ± 0.1	3.9 ± 0.1
	75	10.9 ± 0.3	8.6 ± 0.2	7.8 ± 0.3	4.3 ± 0.1	–	–	–	–	3.1 ± 0.2	4.3 ± 0.1
	100	10.4 ± 0.2	8.4 ± 0.2	7.4 ± 0.2	4.4 ± 0.2	4.2 ± 0.2	2.7 ± 0.1	3.3 ± 0.2	2.1 ± 0.1	3.0 ± 0.1	4.0 ± 0.1
	150	9.7 ± 0.2	7.6 ± 0.2	6.6 ± 0.2	3.3 ± 0.1	–	–	–	–	3.1 ± 0.1	4.3 ± 0.2
	200	9.7 ± 0.3	7.7 ± 0.2	8.1 ± 0.3	4.2 ± 0.2	4.0 ± 0.2	2.0 ± 0.1	3.7 ± 0.2	2.5 ± 0.1	1.6 ± 0.1	3.5 ± 0.1

[a] Unit = dpm/100 L.

Then, the residence times were calculated using the following equation:

$$\tau = \frac{I}{F^x} \quad (6)$$

where τ represents the residence time of ^{210}Po, and F^x is the removal flux of the total dissolved, truly dissolved, colloidal, or particulate phase of ^{210}Po (K, P, J, C, and S_c, respectively). In the upper layer (0–100 m), the residence times of the truly dissolved, colloidal, and particulate phases of ^{210}Po were in the ranges of 46–121 days (avg.: 92 days), 45–93 days (avg.: 77 days), and 79–201 days (avg.: 129 days), respectively.

However, this sequential scavenging model neglects biological uptake from the dissolved phase to the particulate phase and remineralization from the particulate phase to the dissolved phase. In order to obtain more reasonable residence times that account for such biological turnovers of ^{210}Po, we used a simple mass balance model (Kim et al., 1999b) for the residence times of the truly dissolved, colloidal, and particulate phases (Fig. 4), which can be represented as follows:

$$\tau_{tot} = \tau_{dis} + \tau_{col} + \tau_{par} \quad (7)$$

$$\tau_{tdis} = \tau_{dis} + \tau_{col} \quad (8)$$

In this model, the residence time of the particulate phase is the difference between the residence times of the total ^{210}Po and the total dissolved ^{210}Po (from eq. (6)). Similarly, the residence time of the colloidal phase is obtained from the difference between the residence times of the total dissolved ^{210}Po and the truly dissolved ^{210}Po (from equation 6).

Applying this net residence time model to the upper 0–100 m layer of the EJS, the residence times of the truly dissolved, colloidal, and particulate phases of ^{210}Po were found to be 92 ± 41, 63 ± 14, and 166 ± 45 days, respectively (Table 3). For the residence times of the colloidal and particulate phases of ^{210}Po, the calculated results of the net residence time model showed differences as great as 30% from those of the sequential scavenging model. This suggests that a general sequential model can underestimate or overestimate the residence times of these isotopes because of their reversible characteristics in the ocean, considering that the uncertainties of each model are less than 10%. These residence times for the total dissolved phase of ^{210}Po agree well with those reported for other oceanic regions (Bacon et al., 1976; Nozaki et al., 1976; Spencer et al., 1980; Cochran et al., 1983; Sarin et al., 1999; Masqué et al., 2002).

According to recent studies, similar to ^{234}Th, ^{210}Po could be a potentially good tracer for POC (Shimmield et al., 1995; Friedrich and Rutgers van der Loeff, 2002; Murray et al., 2005; Stewart et al., 2010). However, previous studies have suggested that the volume concentration factors of ^{210}Po in phytoplankton are different for different species (Stewart and Fisher, 2003a) and that the assimilation rates of the ingested ^{210}Po in copepods were in the range of 19–55% depending on phytoplankton diets (Stewart and Fisher, 2003b). In addition, nitrogen fixation is disproportionally important in the removal of ^{210}Po in seawater (Kim, 2001). Thus, a careful examination of the relationships between POC/^{210}Po ratios in particles and ^{210}Po deficiencies is necessary for each study region in order to utilize ^{210}Po as a tracer of POC in the ocean as suggested by Verdeny et al. (2009).

The colloidal residence times of ^{210}Po were several fold longer than those of ^{234}Th (<10 days for 10 kDa–0.20 or 0.45 μM) in the Sargasso Sea (Moran and Buesseler, 1992), in the northeast Pacific Ocean (Huh and Prahl, 1995), and in the Gulf of Mexico (Guo et al., 1997), even if the differences in oceanographic conditions are considered. These colloidal ^{234}Th residence times agree well with the turnover time of high-molecular-weight (HMW) dissolved organic matter (DOM) (Amon and Benner, 1994). The deficiencies of truly dissolved and colloidal ^{210}Po relative to ^{210}Pb showed a significant positive correlation ($r^2 = 0.7$) with the DOC concentrations in the upper 0–100 m layer (Fig. 3). These correlations show that the residence times of truly dissolved and colloidal ^{210}Po in the euphotic zone are closely linked to DOC production/cycling. However, these much longer colloidal residence times of ^{210}Po relative to ^{234}Th and HMW-DOM (obtained under various oceanographic conditions) indicate that Po turns over several times through HMW-DOM before settling down from the euphotic zone since all elements in colloids should turn over together by bacterial degradation or by aggregation.

The residence times of total ^{210}Po in this study were similar to those of some bio-reactive trace elements, such as Co (290 days) and Ni (1 year) estimated using sediment traps in the surface water of the South China Sea (Ho et al., 2010). In addition, the proportions of the colloidal phase to the total dissolved phase were $58 \pm 5\%$ for ^{210}Pb and $65 \pm 5\%$ for ^{210}Po in the EJS, which were similar to those found for stable Pb (60%), Cu (50%), and Mn (55%) in the Venice Lagoon (Martin et al., 1995), despite the difference in oceanic conditions, but were much larger than ^{234}Th (<10%) in the Sargasso Sea (Moran and Buesseler, 1992). Thus, our study suggests that colloidal ^{210}Po is potentially a good tracer for the turnover rate of some bio-reactive elements through HMW-DOM in the euphotic zone.

Table 3
Residence times (days) of ^{210}Po based on the reversible scavenging model in the surface layer of the East/Japan Sea.

Location	Depth (m)	Total	Total dissolved (<0.45 μm)	Truly dissolved (<10 kDa)	Colloid (10 kDa–0.45 μm)	Particulate (>0.45 μm)
S1	0–100	319	182	110	72	137
S2	0–100	259	116	46	70	143
S3	0–100	386	168	121	47	218

4. CONCLUSIONS

The residence times of colloidal ^{210}Po estimated using the net residence time model were in the range of 47–72 days, which were much longer than those of ^{234}Th and HMW-DOM in the surface ocean. Such long colloidal residence times for ^{210}Po, relative to ^{234}Th indicate that Po, together with some proxy bio-reactive elements, turns over several times through HMW-DOM before they settle down from the euphotic zone. Thus, our results suggest that colloidal ^{210}Po is potentially used as an excellent tracer for studying the roles of colloids in the removal and cycling of some bio-reactive elements in the ocean. More extensive studies are necessary in order to elucidate the link between Po and other bio-reactive elements in DOM cycling.

ACKNOWLEDGEMENTS

We would like to thank I. T. Kim for helping with field sampling. This research was a part of the project titled "East Asian Seas Time series-I (EAST-I)" funded by The Ministry of Land, Transport and Maritime Affairs, Korea and The "National Research Foundation of Korea (NRF)" grant funded by The Korea government (MEST) (No. 2012-0006256). THK was partially supported by the BK21 scholarship from the School of Earth and Environmental Sciences, Seoul National University, Korea.

REFERENCES

Amon R. M. W. and Benner R. (1994) Rapid cycling of high-molecular-weight dissolved organic matter in the ocean. *Nature* **369**, 549–552.

Bacon M. P., Belastock R. A., Tecotzky M. and Turekian K. K. (1988) Lead-210 and polonium-210 in ocean water profiles of the continental shelf and slope south of New England. *Cont. Shelf Res.* **8**, 841–853.

Bacon M. P., Spencer D. W. and Brewer P. G. (1976) Pb-210/Ra-226 and Po-210/Pb-210 disequilibria in seawater and suspend particulate matter. *Earth Planet. Sci. Lett.* **32**, 277–296.

Baskaran M., Swarzenski P. W. and Porcelli D. (2003) Role of colloidal material in the removal of ^{234}Th in the Canada basin of the Arctic Ocean. *Deep-Sea Res. I* **50**, 1353–1373.

Carlson C. A. and Ducklow H. W. (1995) Dissolved organic carbon in the upper ocean of the central equatorial Pacific ocean, 1992: daily and finescale vertical variations. *Deep-Sea Res. II* **42**, 639–656.

Cherry R. D., Fowler S. W., Beasley T. M. and Heyraud M. (1975) Polonium-210: its vertical oceanic transport by zooplankton metabolic activity. *Mar. Chem.* **3**, 105–110.

Chung Y. (1987) ^{210}Pb in the western Indian Ocean: distribution, disequilibrium, and partitioning between dissolved and particulate phases. *Earth Planet. Sci. Lett.* **85**, 28–40.

Chung Y. and Craig H. (1983) ^{210}Pb in the Pacific: the GEOSECS measurements of particulate and dissolved concentrations. *Earth Planet. Sci. Lett.* **65**, 406–432.

Chung Y. and Finkel R. (1988) ^{210}Po in the western Indian Ocean: distribution, disequilibrium, and partitioning between dissolved and particulate phases. *Earth Planet. Sci. Lett.* **88**, 232–240.

Chung Y. and Wu T. (2005) Large ^{210}Po deficiency in the northern South China Sea. *Cont. Shelf Res.* **25**, 1209–1224.

Coale K. H. and Bruland K. W. (1987) Oceanic stratified euphotic zone as elucidated by ^{234}Th:^{238}U disequilibria. *Limnol. Oceanogr.* **32**, 189–200.

Cochran J. K., Bacon M., Krishnaswami S. and Turekian K. (1983) ^{210}Po and ^{210}Pb distributions in the central and eastern Indian Ocean. *Earth Planet. Sci. Lett.* **17**, 295-273.

Fisher N. S., Burns K. A., Cherry R. D. and Heyraud M. (1983) Accumulation and cellular distribution of ^{241}Am, ^{210}Po, and ^{210}Pb in two marine algae. *Mar. Ecol. Prog. Ser.* **11**, 233–237.

Fowler S. W. and Knauer G. A. (1986) Role of large particles in the transport of elements and organic compounds through the oceanic water column. *Prog. Oceanogr.* **16**, 147–194.

Friedrich, J. and Rutgers van der Loeff, M. (2002) A two tracer (^{210}Po–^{234}Th) to distinguish organic carbon and biogenic silica export flux in the Antarctic Circumpolar Current. Deep-Sea Res. 49, 101–120.

Gamo T., Momoshima N. and Tolmachyov S. (2001) Recent upward shift of the deep convection system in the Japan Sea, as inferred from the geochemical tracers tritium, oxygen, and nutrients. *Geophys. Res. Lett.* **28**(21), 4143–4146.

Gueguen C., Belin C. and Dominik J. (2002) Organic colloid separation in contrasting aquatic environments with tangential flow filtration. *Water Res.* **36**, 1677–1684.

Guo L. and Santschi P. H. (1996) A critical evaluation of the cross-flow ultrafiltration technique for sampling colloidal organic carbon in seawater. *Mar. Chem.* **55**, 113–127.

Guo L. and Santschi P. H. (1997) Composition and cycling of colloids in marine environments. *Rev. Geophys.* **35**, 17–40.

Guo L., Santschi P. H. and Baskaran M. (1997) Interactions of thorium isotopes with colloidal organic matter in oceanic environments. *Colloids Surf. A* **120**, 255–271.

Hansell D. A. and Carlson C. A. (1998) Net community production of dissolved organic carbon. *Global Biogeochem. Cycles* **12**, 443–453.

Ho T.-Y., Chou W.-C., Wei C.-L., Lin F.-J., Wong G. T. F. and Lin H.-L. (2010) Trace metal cycling in the surface water of the South China Sea: Vertical fluxes, composition, and sources. *Limnol. Oceanogr.* **55**, 1807–1820.

Hong C. H. and Cho K. D. (1983) The Northern boundary of the Tsushima Current and its Fluctuations. *J. Oceanol. Soc. Korea* **18**, 1–9.

Huh C. A. and Prahl F. G. (1995) Role of colloids in upper ocean biogeochemistry in the northeast Pacific Ocean elucidated from ^{238}U–^{234}Th disequilibria. *Limnol. Oceanogr.* **40**(3), 528–532.

Jo C. O., Lee J. Y., Park K. A., Kim Y. H. and Kim K. R. (2007) Asian dust initiated early spring bloom in the northern East/Japan Sea. *Geophys. Res. Lett.* **34**, L05602. http://dx.doi.org/10.1029/2006GL027395.

Kadko D. (1993) Excess ^{210}Po and nutrient cycling within the California coastal transition zone. *J. Geophys. Res.* **98**, 857–864.

Kim G. (2001) Large deficiency of polonium in the oligotrophic oceans interior. *Earth Planet. Sci. Lett.* **192**, 15–21.

Kim G. and Church T. M. (2001) Seasonal biogeochemical fluxes of ^{234}Th and ^{210}Po in the upper Sargasso Sea: influence from atmospheric iron deposition. *Global Biogeochem. Cycles* **15**, 651–661.

Kim G., Hussain N., Church T. M. and Yang H.-S. (1999a) A practical and accurate method for the determination of 234Th simultaneously with ^{210}Po and ^{210}Pb in seawater. *Talanta* **49**, 851–858.

Kim G., Hussain N. and Church T. M. (1999b) How accurate are the ^{234}Th based particulate residence times in the ocean? *Geophys. Res. Lett.* **26**, 619–622.

Kim K.-R., Kim G., Kim K., Lobanov V., Ponomarev V. and Salyuk A. (2002) A sudden bottom-water formation during the severe winter 2000–2001. The case of the East/Japan. *Sea Geophys. Res. Lett.* **29**(8), 75–78.

Kim K., Kim K.-R., Min D.-H., Volkov Y., Yoon J.-H. and Takematsu M. (2001) Warming and Structural Changes in the

East (Japan) Sea: A Clue to Future Changes in Global Oceans? Geophys. *Res. Lett.* **28**, 3293–3296.

Kim T.-H., Lee Y. W. and Kim G. (2010) Hydrographically mediated patterns of photosynthetic pigments in the East/Japan Sea: Low N:P ratios and cyanobacterial dominance. *J. Mar. Syst.* **82**, 72–79.

Martin J.-M., Dai M.-H. and Cauwet G. (1995) Significance of colloids in the biogeochemical cycling of organic carbon and trace metals in a coastal environment – Example of the Venice Lagoon (Italy). *Limnol. Oceanogr.* **40**, 119–131.

Masqué P., Sanchez–Cabeza J. A., Bruach J. M., Palacios E. and Canals M. (2002) Balance and residence times of Pb-210 and Po-210 in surface waters of the Northwestern Mediterranean Sea. *Cont. Shelf Res.* **22**, 2127–2146.

Moran S. B. and Buesseler K. O. (1992) Short residence time of colloids in the upper ocean estimated from 238U–234Th disequilibria. *Nature* **359**, 221–223.

Murray J. W., Paul B., Dunne J. P. and Chapin T. (2005) ^{234}Th, ^{210}Pb, ^{210}Po and stable Pb in the central equatorial Pacific: tracers for particle cycling. *Deep-Sea Res. I* **52**, 2109–2139.

Nozaki Y., Thomson J. and Turekian K. K. (1976) The distribution of ^{210}Pb and ^{210}Po in the surface waters of the Pacific Ocean. *Earth Planet. Sci. Lett.* **32**, 304–312.

Nozaki Y., Ikuta N. and Yashima M. (1990) Unusually large ^{210}Po deficiencies relative to ^{210}Pb in the Kuroshio Current of the East China and Philippine Seas. *J. Geophys. Res.* **95**, 5321–5329.

Nozaki Y., Zhang J. and Takeda A. (1997) ^{210}Pb and ^{210}Po in the equatorial Pacific and the Bering Sea: the effects of biological productivity and boundary scavenging. *Deep-Sea Res.* **44**, 2203–2220.

Park K.-A., Chung J. Y. and Kim K. (2004) Sea surface temperature fronts in the East (Japan) Sea and temporal variations. *Geophys. Res. Lett.*, 31:10.1029/2004GL019424.

Rebstock G. A. and Kang Y. S. (2003) A comparison of three marine ecosystems surrounding the Korean peninsula: responses to climate change. *Prog. Oceanogr.* **59**, 357–379.

Sarin M. M., Kim G. and Church T. M. (1999) ^{210}Po and ^{210}Pb in the south-equatorial Atlantic: distribution and disequilibria in the upper 500 m. *Deep-Sea Res. II* **46**, 907–917.

Shimmield G. B., Ritchie G. D. and Fileman T. W. (1995) The impact of marginal ice zone processes on the distribution of ^{210}Pb, ^{210}Po, and ^{234}Th and implications for new production in the Bellingshausen Sea, Antarctica. *Deep-Sea Res. II* **42**, 1313–1335.

Spencer D. W., Bacon M. P. and Brewer P. G. (1980) The distribution of Pb-210 and Po-210 in the North Sea. *Thalassia Jugosl.* **16**, 125–154.

Stewart G. M. and Fisher N. S. (2003a) Experimental studies on the accumulation of polonium-210 by marine phytoplankton. *Limnol. Oceanogr.* **48**, 1193–1201.

Stewart G. M. and Fisher N. S. (2003b) Bioaccumulation of polonium-210 in marine copepods. *Limnol. Oceanogr.* **48**, 2011–2019.

Stewart G. M., Fowler S. W., Teyssie J.-L., Cotret O., Cochran J. K. and Fisher N. S. (2005) Contrasting transfer of polonium–210 and lead–210 across three trophic levels in marine plankton. *Mar. Ecol. Prog. Ser.* **290**, 27–33.

Stewart G. M., Moran S. B. and Lomas M. W. (2010) Seasonal POC fluxes at BATS estimated from ^{210}Po deficits. *Deep-Sea Res. I* **57**, 113–124.

Tsunogai, S., Watanabe, Y. W., Harada, K., Watanabe, S., Saito, S. and Nakajima, M. (1993) Dynamics of the Japan Sea deep water studied with chemical and radiochemical tracers. In Deep Ocean Circulation, Physical and Shemical Aspect, (eds. T. Teramoto). Elsevier Science Publishers, B.V. pp. 105-119.

Verdeny E., Masqué P., Garcia-Orellana J., Hanfland C., Cochran J. K. and Stewart G. M. (2009) POC export from ocean surface waters by means of ^{234}Th/^{238}U and ^{210}Po/^{210}Pb disequilibria: a review of the use of two radiotracer pairs. *Deep-Sea Res. II* **56**, 1502–1518.

Wei C.-L. and Murray J. W. (1994) The behavior of scavenged isotopes in marine anoxic environments: ^{210}Pb and ^{210}Po in the water column of the Black Sea. *Geochim. Cosmochim. Acta* **58**, 1795–1811.

Wright S. W., Jeffrey S. W., Mantoura R. F. C., Llewellyn C. A., Bjørnland T., Repeta D. and Welschmeyer N. (1991) Improved HPLC method for the analysis of chlorophylls and carotenoids from marine phytoplankton. *Mar. Ecol. Prog. Ser.* **77**, 183–196.

Associate editor: S. Krishnaswami